Pure Appl. Geophys. 170 (2013), 1661–1671

DOI 10.1007/s00024-012-0510-8

Pure and Applied Geophysics

Analytical Solutions for Tsunami Waves Generated by Submarine Landslides in Narrow Bays and Channels

IRA DIDENKULOVA[1,2] and EFIM PELINOVSKY[2,3,4]

Abstract—Analytical theory of tsunami wave generation by submarine landslides is extended to the case of narrow bays and channels of different geometry, in the shallow-water theory framework. New analytical solutions are obtained. For a number of bottom configurations, the wave field can be found explicitly in the form of the Duhamel integral. It is described by three waves: one forced wave propagating together with the landslide and two free waves propagating in opposite directions. The cases for bays with triangular (V-shaped bay), parabolic (U-shaped bay), and rectangular cross-sections are discussed in detail. The dynamics of the offshore-propagating wave in linearly inclined bays of different cross-section are also studied asymptotically for the resonant moving landslide. Different cases of landslides of increasing and decreasing volume are considered. It is shown that even if the landslide is moving under fully resonant conditions, the amplitude of the propagating tsunami wave may still be bounded, depending on the type of the landslide.

Key words: Tsunami, landslides, bays and channels, shallow water theory.

1. Introduction

Landslide motions and rock failures are now recognized as important sources of tsunami waves (KEATING *et al.*, 2000; BARDET *et al.*, 2003; YALCINER *et al.*, 2003; GUSIAKOV, 2009). A list of examples includes the Papua New Guinea tsunami of 17 July 1998 (MCSAVENEY *et al.*, 2000; SYNOLAKIS *et al.*, 2002), the tsunami in Izmit Bay (Turkey) of 17 August 1999 (ALTINOK *et al.*, 2001), the tsunami in Fatu Hiva (Marquesas islands; French Polynesia) of 13 September 1999 (OKAL *et al.*, 2002), the Stromboli tsunami of 30 December 2002 (TINTI *et al.*, 2006), a possible landslide tsunami of 7 May 2007 in the Black Sea (RANGUELOV *et al.*, 2008), and the largest known tsunami event in Lituya Bay of 9 July 1958 (FRITZ *et al.*, 2009).

To describe landslide tsunami generation, a variety of numerical models have been used (HARBITZ *et al.*, 1993; IMAMURA and GICA, 1996; HEINRICH *et al.*, 1999; ASSIER-RZADKIEWICZ *et al.*, 2000; MANGENEY *et al.*, 2000; FINE *et al.*, 2005; LIU *et al.*, 2005; TINTI *et al.*, 2006; KUO *et al.*, 2008; among others). Fewer analytical methods are available. Most are limited to the one-dimensional (1D) case of landslide motion in the shallow-water approximation (PELINOVSKY, 1996; TINTI and BORTOLUCCI, 2000; TINTI *et al.*, 2001; LIU *et al.*, 2003; OKAL and SYNOLAKIS, 2003). For 2D and 3D cases, we note the works by (NOVIKOVA and OSTROVSKY, 1978; PELINOVSKY and POPLAVSKY, 1996; WARD, 2001; DI RISIO and SAMMARCO, 2008; SAMMARCO and RENZI, 2008). The 2D shallow-water model by (SAMMARCO and RENZI, 2008) also describes the generation and propagation of edge waves induced by a landslide of constant volume.

In all models above the volume of the landslide is conserved. However, landslide and avalanche motion are often accompanied by erosive and accretive processes, which lead to variations of the landslide volume (PUDASAINI and HUTTER, 2007). The first analysis of tsunami wave generation from a landslide of varying volume was performed by (DIDENKULOVA *et al.*, 2010) for two specific 1D bottom profiles $h \sim x^{4/3}$ (h is the water depth and x is coordinate directed offshore) and $h \sim x^4$. These two bottom profiles enable presentation of the general solution as a superposition of two travelling waves propagating

[1] Laboratory of Wave Engineering, Institute of Cybernetics, Tallinn, Estonia. E-mail: ira@cs.ioc.ee
[2] Department of Applied Mathematics, Nizhny Novgorod State Technical University, Nizhny Novgorod, Russia.
[3] Department of Nonlinear Geophysical Processes, Institute of Applied Physics, Nizhny Novgorod, Russia.
[4] Higher School of Economics, Nizhny Novgorod, Russia.

in opposite directions (Didenkulova *et al.*, 2009; Didenkulova and Pelinovsky, 2010).

This paper extends work by (Didenkulova *et al.*, 2010) to the 2D case of U and V-shaped bays and channels, taking into account the variability of landslide volume. It is organized as follows. The basic shallow-water model, and specification of studied basic bay geometries are described in the Sect. 2. Rigorous solutions for tsunami wave generation by landslide motion along these bays are obtained in the Sect. 3, where bays of triangular (V-shaped), parabolic (U-shaped), and rectangular cross-section are discussed in detail. The resonant motion of landslides of varying volume along inclined channels of different cross-section is studied in the Sect. 4. The main results are summarized in the Sect. 5.

2. *Basic Model of Landslide Tsunami Generation in U-Shaped Bays*

The propagation and runup of long waves in V and U-shaped bays and channels has been studied by (Didenkulova and Pelinovsky, 2009, 2011a, b). The governing equations for tsunami wave generation by underwater landslides in narrow bays and channels can be written similar to the 1D case studied in (Pelinovsky, 1996; Tinti *et al.*, 2001; Liu *et al.*, 2003; Didenkulova *et al.*, 2010):

$$\frac{\partial S}{\partial t} + \frac{\partial}{\partial x}[Su] = \frac{\partial S_b}{\partial t}, \qquad (1)$$

$$\frac{\partial u}{\partial t} + u\frac{\partial u}{\partial x} + g\frac{\partial \eta}{\partial x} = 0, \qquad (2)$$

where $\eta(x,t)$ is the sea surface elevation, $u(x, t)$ is the flow velocity averaged over a cross-section, g is the acceleration due to gravity, $S(\eta,x,t)$ is the variable cross-section of the bay, $S_b(x, t)$ describes the landslide motion, x is coordinate directed offshore, and t is time. Generated waves and landslide body are assumed to be uniform over the cross-section (Fig. 1).

In the case of an inclined bay with a cross-section described by the power law $z \sim |y|^m$, m is a cross-section factor, which can be any positive number, the variable cross-section of the bay $S(\eta,x,t)$ is related to the total water depth of the main bay axis $H = h(x) + \eta(x, t)$ as $S \sim H^q$, where $q = \frac{m+1}{m}$, and

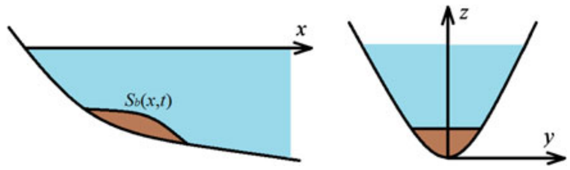

Figure 1
The geometry of the problem: a uniform sea surface elevation over the cross-section, $\eta(x, t)$, is generated by a landslide with the shape $S_b(x, t)$

Eqs. (1) and (2) can be re-written in terms of the total water depth:

$$\frac{\partial H}{\partial t} + u\frac{\partial H}{\partial x} + \frac{H}{q}\frac{\partial u}{\partial x} = \frac{\partial z_b}{\partial t}, \quad \frac{\partial u}{\partial t} + u\frac{\partial u}{\partial x} + g\frac{\partial H}{\partial x} = g\frac{dh}{dx}, \qquad (3)$$

where $z_b(x,t)$ is the moving bottom boundary along the main channel axis, which is assumed to be constant over the channel cross-section. Analytical solutions for tsunami wave generation by the moving landslide can be obtained by linear approximation, and the linearized equation Eq. (3) take the form:

$$\frac{\partial \eta}{\partial t} + u\frac{dh}{dx} + \frac{h}{q}\frac{\partial u}{\partial x} = \frac{\partial z_b}{\partial t}, \quad \frac{\partial u}{\partial t} + g\frac{\partial \eta}{\partial x} = 0. \qquad (4)$$

Finally, Eq. (4) can be transformed to Eq. (5) for sea surface elevation:

$$\frac{\partial^2 \eta}{\partial t^2} - g\frac{dh}{dx}\frac{\partial \eta}{\partial x} - \frac{gh}{q}\frac{\partial^2 \eta}{\partial x^2} = \frac{\partial^2 z_b}{\partial t^2}. \qquad (5)$$

Initial conditions for the shallow-water system (Eqs. 1 and 2) are applied to both $\eta(x,t)$ and $u(x, t)$. If, at the initial moment the ocean rests and the landslide starts its motion instantaneously, the effective initial conditions have the following form (Didenkulova *et al.*, 2010):

$$\eta(x,0) = z_b(x,0), \quad \frac{\partial \eta}{\partial t}(x,0) = \frac{\partial z_b}{\partial t}(x,0). \qquad (6)$$

Initial conditions for this type are similar to those known for tsunami generation by earthquakes. This similarity comes from the fact that at one moment the landslide is stationary and the next moment it abruptly starts its motion along the slope. These initial conditions (Eq. 6) for tsunami generation by landslides have been rigorously derived and discussed in detail by (Didenkulova *et al.*, 2010).

Equation (5) is an inhomogeneous wave equation with variable coefficients which cannot be solved analytically in the general case. That is why we seek specific conditions when this equation can be reduced to an inhomogeneous constant-coefficient equation. For this purpose, we apply the transformation similar to that which was used to find nonreflecting bottom configurations (Didenkulova *et al.*, 2008, 2009; Grimshaw *et al.*, 2010):

$$\eta = A(x)Y(\tau(x), t). \tag{7}$$

Substituting Eq. (7) into Eq. (5) we obtain a so-called inhomogeneous Klein-Gordon equation:

$$A\left\{\frac{\partial^2 Y}{\partial t^2} - \frac{gh}{q}\left(\frac{d\tau}{dx}\right)^2 \frac{\partial^2 Y}{\partial \tau^2}\right\} - \frac{\partial Y}{\partial \tau}\left\{gA\frac{dh}{dx}\frac{d\tau}{dx} + 2\frac{gh}{q}\frac{dA}{dx}\frac{d\tau}{dx} + A\frac{gh}{q}\frac{d^2\tau}{dx^2}\right\} - Y\left\{g\frac{dh}{dx}\frac{dA}{dx} + \frac{gh}{q}\frac{d^2A}{dx^2}\right\} = \frac{\partial^2 z_b}{\partial t^2} \tag{8}$$

The first term in Eq. (8) is a standard wave operator (d'Alembertian) if:

$$\left(\frac{d\tau}{dx}\right)^2 = \frac{q}{gh(x)}. \tag{9}$$

Equation (9) defines the travel time of wave propagation in the channel $\tau = \int dx/c$ with the speed $c(x) = \sqrt{gh/q}$. The coefficient after $\frac{\partial Y}{\partial \tau}$ (the second term in Eq. 8) should be equal to zero in order to satisfy the boundedness of the wave field,

$$gA\frac{dh}{dx}\frac{d\tau}{dx} + 2\frac{gh}{q}\frac{dA}{dx}\frac{d\tau}{dx} + A\frac{gh}{q}\frac{d^2\tau}{dx^2} = 0. \tag{10}$$

Equations (10) and (9) gives us the generalized Green's law for wave propagation in channels of variable depth and cross-section (Mei, 1989; Synolakis, 1991; Didenkulova and Pelinovsky, 2011a):

$$Ah^{\frac{2q-1}{4}} = \text{const.} \tag{11}$$

And, finally, to obtain the constant-coefficient wave equation, the last term in Eq. (8) should also be equal to zero:

$$g\frac{dh}{dx}\frac{dA}{dx} + \frac{gh}{q}\frac{d^2A}{dx^2} = 0. \tag{12}$$

Taking into account Eq. (11), Eq. (12) gives us a set of specific bay geometries:

$$h \sim x^{\frac{4}{2q+1}}, \quad S(x) \sim h^q. \tag{13}$$

These bay geometries, which induce wave propagation over large distances without energy loss, were discussed extensively by (Didenkulova and Pelinovsky, 2011a).

Thus, the final expression for the basic equation describing tsunami wave generation by landslides in inclined bays and channels is:

$$\frac{\partial^2 Y}{\partial t^2} - \frac{\partial^2 Y}{\partial \tau^2} = \frac{\partial^2}{\partial t^2}\left(\frac{z_b(\tau, t)}{A(\tau)}\right), \tag{14}$$

where $A(\tau)$ is fully determined for each channel configuration by use of Eqs. (11) and (13). Equation (14) is an inhomogeneous wave equation, which can be solved analytically, as demonstrated in the next section.

3. *Tsunami Generation by Landslide Motion Along the Bay*

The solution of Eq. (14) satisfying the initial conditions in Eq. (6) can be expressed in the form of the Duhamel integral (Courant and Hilbert, 1989):

$$Y(\tau, t) = \frac{1}{2}\left[\frac{z_b(\tau - t)}{A(\tau - t)} + \frac{z_b(\tau + t)}{A(\tau + t)}\right] + \frac{1}{2}\int_{\tau - t}^{\tau + t} \frac{1}{A(\sigma)}\frac{\partial z_b}{\partial t}(\sigma, 0)d\sigma + \frac{1}{2}\int_0^t d\rho \int_{\tau-(t-\rho)}^{\tau+(t-\rho)} \frac{1}{A(\varsigma)}\frac{\partial^2 z_b}{\partial \rho^2}(\varsigma, \rho)d\varsigma. \tag{15}$$

Equation (15) does not imply any restriction of the properties of the landslide and its speed; it can be used to study different types of landslide motion, including variable volume of the landslide body and variable speed of landslide motion. The solution of Eq. (15) can be found in the explicit form if the landslide moves as:

$$z_b(\tau, t) = A(\tau)Z(\tau - Fr \cdot t), \tag{16}$$

where the Froude number:

$$Fr = \frac{V(x)}{c(x)}, \tag{17}$$

is constant and determines the variable speed of the landslide in the basin of variable depth.

Equation (15) for the special landslide shape (Eq. 16) transforms into:

$$\eta(x,t) = \frac{Fr^2}{Fr^2 - 1} A(x) Z\left[\int_0^x \frac{dx'}{c(x')} - Fr\cdot t\right] - \frac{A(x)}{2(Fr-1)} Z\left[\int_0^x \frac{dx'}{c(x')} - t\right] + \frac{A(x)}{2(Fr+1)} Z\left[\int_0^x \frac{dx'}{c(x')} + t\right], \tag{18}$$

and represents three waves. The first term describes the forced wave, which propagates together with the landslide. Its length increases with increasing distance and its amplitude is proportional to the thickness of the landslide and decreases with a distance. The forced wave can have different polarity, depending on the type of the landslide motion. It is positive in the super-critical range ($Fr > 1$) and negative in the sub-critical range ($Fr < 1$). The second term describes a free wave, which propagates with the speed $c(x)$. As for the forced wave, it can also be of different polarity: negative in the super-critical range and positive in the sub-critical range. The last term corresponds to the free wave of positive polarity propagating onshore.

It is important to mention that the solution of Eq. (18) has the same form for waves generated by a landslide moving with constant speed in a basin of constant depth (Tinti *et al.*, 2001; Pelinovsky, 1996; Okal and Synolakis, 2003) and for a 1D landslide moving along a non-reflecting bottom profile $h \sim x^{4/3}$ (Didenkulova *et al.*, 2010). The limitations of constant landslide speed and constant Froude number discussed above are not adequate physically, but they are the only ones that enable analytical solution of the problem. It is also important to note that the general structure of the wave field remains qualitatively similar even for cases when the speed of the landslide and the Froude number vary arbitrarily (Tinti *et al.*, 2001; Liu *et al.*, 2003; Didenkulova *et al.*, 2011).

The forced wave propagating offshore has a sign-variable shape in the resonant case ($Fr = 1$). This follows from two first terms in Eq. (18) using l'Hôpital's rule. Taking into account that in the vicinity of the resonance $\tau(x) \approx t$, the resonant wave can be written as:

$$\eta_{\mathrm{res}}(x,t) = -\frac{A(x)\tau(x)}{2}\frac{\partial Z}{\partial \tau}[\tau(x) - t]. \tag{19}$$

By use of Eqs. (9), (11), and (13) it can be shown that $A(x)\tau(x)$ tends to a constant asymptotic value for any non-reflecting bay geometry. So, in contrast with the basin of constant depth, where the resonance leads to infinite growth of the wave amplitude, the resonance effect in a basin of a variable depth can be bounded for any kind of non-reflecting beach profile. So, the effectiveness of the resonance decreases because of the decrease in the landslide thickness and wave propagation to deeper water. Of course, this is a very particular solution, which enables rigorous analytical investigation of resonant tsunami wave generation. However, a more general case of landslides of different volume and different bottom structures is discussed in the next section.

Let us study in more detail tsunami wave generation in bays of different cross-sections described by Eq. (18). In particular, wave dynamics in a V-shaped bay ($m = 1$, $q = 2$, $h \sim x^{4/5}$) are calculated below for the initial landslide shape, described by:

$$z_b(x, t=0) = \frac{A(x)}{2}\left[\tanh\left(\frac{\tau(x) - \tau_0 + T/2}{a}\right) - \tanh\left(\frac{\tau(x) - \tau_0 - T/2}{a}\right)\right], \tag{20}$$

where $T = 40$ s, a is a smoothing parameter ($a = 0.3$ T), and $\tau_0 = 5.3$ min, providing the location of a 1.3 km long and 1 m high landslide at a distance of 3 km offshore at a water depth of 50 m. The results of the calculation are presented in Fig. 2, for two different types of wave motion: subcritical ($Fr = 0.7$) and supercritical ($Fr = 1.3$).

For supercritical wave motion ($Fr = 1.3$), the forced wave described by the first term in Eq. (18) represents the leading wave of elevation. For subcritical wave motion ($Fr = 0.7$), it is the second wave of depression moving offshore. Waves propagating offshore become longer (Fig. 2). The variations of

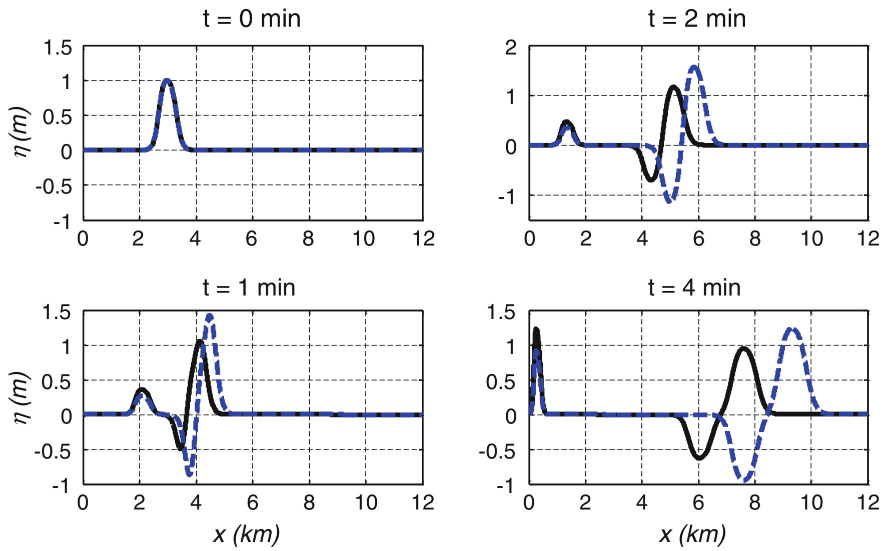

Figure 2
Wave dynamics in a bay of triangular cross-section ($m = 1$), for subcritical (*black solid line*) and supercritical (*blue dashed line*) types of wave motion

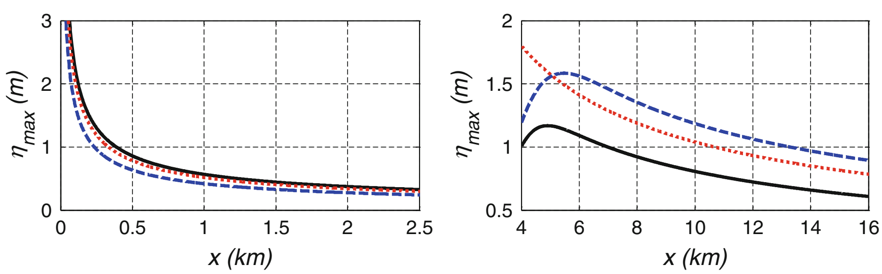

Figure 3
Maximum amplitude of tsunami waves during propagation in a bay of triangular cross-section ($m = 1$) under subcritical (*black solid line*) and supercritical (*blue dashed line*) conditions for waves propagating onshore (*left*) and offshore (*right*); the *red dotted line* corresponds to the generalized Green's law (Eq. 11)

their amplitudes are presented in Fig. 3. In the beginning, for a short time, amplitudes of individual waves propagating offshore are increased by the resonant effect up to the factor of 1.5 in the case of supercritical wave motion but at a distance of about 2–3 wavelengths they start to be determined by the generalized Green's law Eq. (11) (Fig. 3).

The onshore-going free wave described by the third term in Eq. (18) moves onshore with a weak initial amplitude that grows when the wave approaches the coast (Fig. 2). The wave approaching the beach increases in amplitude according to the Green's law (Fig. 3) and reduces in length. The wave amplitude is higher under subcritical conditions than under supercritical conditions. The shoaling effect becomes significant near the shore and results in significant wave amplification.

The dynamics of the waves induced by a similar initial landslide (Eq. 20) ($T = 40$ s, $\tau_0 = 5.5$ min) located at the same distance offshore (3 km) and at the same water depth (50 m) in the U-shaped ($m = 2$, $q = 3/2$, $h \sim x$) bay are displayed in Fig. 4. Generally, the wave dynamics are the same as for the V-shaped bay, but waves in U-shaped bay ($m = 2$) propagate more quickly than in the V-shaped ($m = 1$). This difference is related to the difference in wave speeds $c(x) = \sqrt{mgh/(m+1)}$. Also, amplitudes of offshore-going waves in U-shaped bays grow

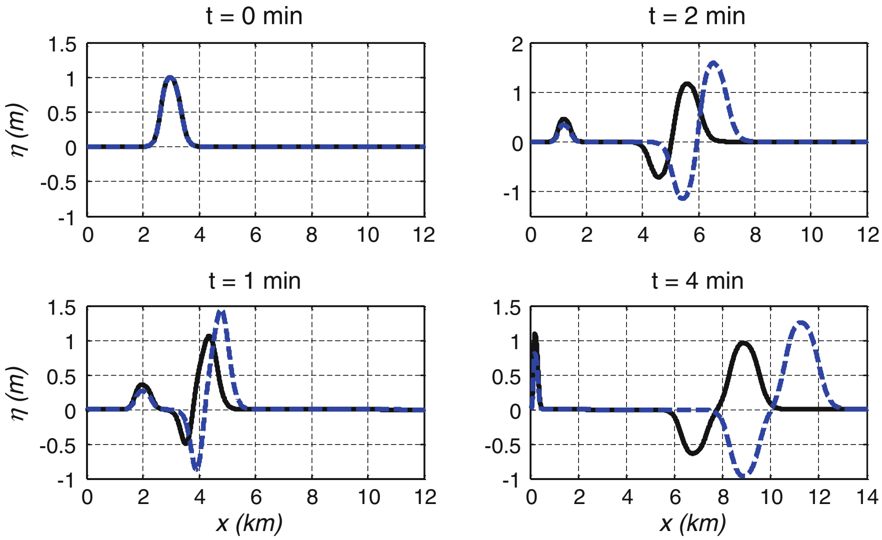

Figure 4
Wave dynamics in a bay of parabolic cross-section ($m = 2$) under subcritical (*black solid line*) and supercritical (*blue dashed line*) conditions

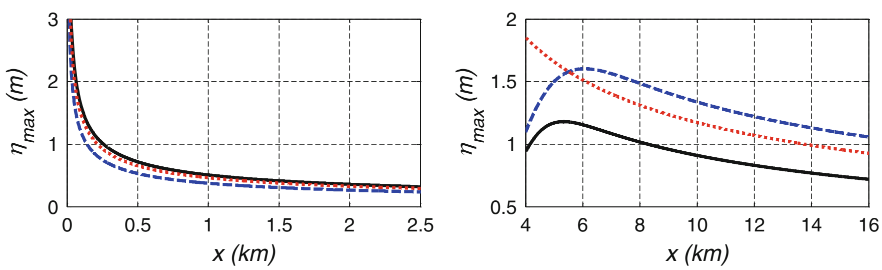

Figure 5
Maximum amplitude of a tsunami wave during its propagation in a bay of parabolic cross-section ($m = 2$) under subcritical (*black solid line*) and supercritical (*blue dashed line*) conditions for waves propagating onshore (*left*) and offshore (*right*); the *red dotted line* corresponds to the generalized Green's law (Eq. 11)

faster than in V-shaped bays and amplitudes of onshore-going waves grow more slowly (Fig. 5). This is in agreement with the water depth variations, which change more slowly in an onshore direction and more quickly in an offshore direction along a U-shaped bay than along a V-shaped bay [Eq. (13)]. It can also be seen that the difference in amplitude between subcritical and supercritical conditions is smaller in the U-shaped bay.

The corresponding dynamics of landslide-generated waves in the inclined channel of rectangular cross-section ($m \to \infty$, $q = 1$, $h \sim x^{4/3}$) are shown in Fig. 6 ($\tau_0 = 6.7$ min, T and location of the failure are the same as in the two previous cases). It can be seen that in rectangular bay waves propagate even more quickly, amplitudes of offshore-going waves become higher, and amplitudes of onshore-going waves grow slower than in the two previous cases (Fig. 7).

4. *Resonant Motion of Landslides of Varying Volume*

As has been shown in the Sect. 3, the resonant wave amplitude in specific non-reflecting bays can be bounded, whereas it tends to infinity if the depth of the basin is constant. This makes it clear that resonance should be considered in a more general case of arbitrary bottom variations, different from specific nonreflecting configurations. This should provide further information about the sensitivity of the results

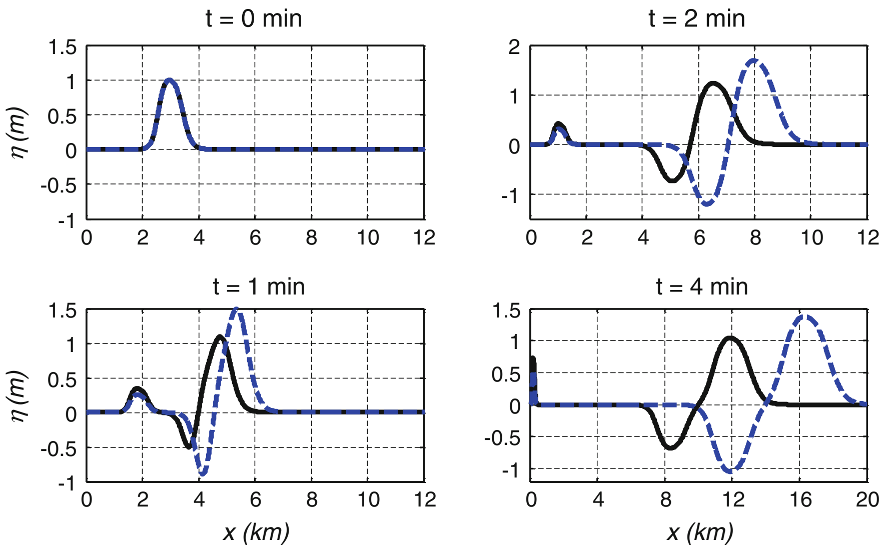

Figure 6
Wave dynamics in a bay of almost rectangular cross-section ($m = 100$) under subcritical (*black solid line*) and supercritical (*blue dashed line*) conditions

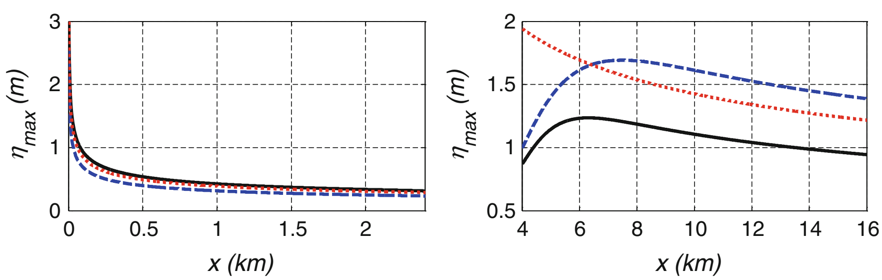

Figure 7
Maximum amplitude of a tsunami wave during its propagation in a bay of almost rectangular cross-section ($m = 100$) under subcritical (*black solid line*) and supercritical (*blue dashed line*) conditions for waves propagating onshore (*left*) and offshore (*right*); the *red dotted line* corresponds to the generalized Green's law (Eq. 11)

obtained to variations of the bottom profile and of landslide characteristics.

Here this effect is studied for a basin of slowly varying depth. We do not analyse the full wave field, because the dynamics of the "non-resonant" wave approaching the coast is not related to the landslide motion (mainly in the initial stage of its motion) and we do not expect large variations of its amplitude for all other conditions of tsunami generation by the landslide. Here we concentrate on "resonant" waves propagating offshore. In the vicinity of the resonance these waves propagate with speeds close to the local wave celerity $c(x)$, which slowly changes with a distance, because the water depth and the cross-section of the bay are slow functions of coordinate x. For this case let us introduce new adequate coordinates in Eq. (5):

$$s = \tau(x) - t, \quad x' = x, \tag{21}$$

where $\tau(x)$ is the travel time as before. After substitution of Eq. (21) the wave equation Eq. (5) has the form:

$$2c(x')\frac{\partial^2\eta}{\partial s \partial x'} + (2q-1)\frac{dc}{dx'}\frac{\partial \eta}{\partial s} = -\frac{\partial^2 z_b}{\partial s^2}, \tag{22}$$

where the term $\partial^2\eta/\partial x^2$ is of the second order of accuracy and can be neglected. Thus, Eq. (22) can be reduced to:

$$\frac{\partial}{\partial x'}\left(c^{q-1/2}\frac{\partial \eta}{\partial s}\right) = -\frac{c^{q-3/2}}{2}\frac{\partial^2 z_b}{\partial s^2}. \quad (23)$$

After integration of Eq. (23) and some simple manipulations, the solution for the sea surface elevation can be found (the prime ($'$) is omitted):

$$\eta(x,s) = -\frac{1}{2c^{q-1/2}}\int_{x_0}^{x} c^{q-3/2}\frac{\partial z_b(y,s)}{\partial s}dy, \quad (24)$$

Equation (24) describes resonant wave propagation in a narrow bay. To satisfy boundary conditions an additional term, describing free non-resonant wave propagation, should be added.

Equation (24) can be used for study of tsunami wave generation by a landslide of a variable volume moving with an arbitrary speed along the bay. It is restricted by the speed of the landslide, which should be close to the wave speed.

Let us consider a resonantly moving landslide of arbitrary shape and variable volume:

$$z_b(x,t) = Q(x)Z(s) = Q(x)Z[\tau(x) - t], \quad (25)$$

which according to Eq. (24) generates tsunami waves of variable amplitude $D(x)$

$$\eta_{res}(x,t) = -D(x)\frac{\partial Z(\tau - t)}{\partial \tau},$$
$$D(x) = \frac{1}{2c^{q-1/2}}\int_{x_0}^{x} c^{q-3/2}Q(y)dy, \quad (26)$$

along a linearly inclined bay

$$h(x) = h_0\frac{x}{x_0}, \quad (27)$$

where x_0 is the initial location of the landslide with the water depth h_0.

As has been mentioned above, to understand all possible types of tsunami wave generation it is important to consider different scenarios of landslide volume variation.

If the landslide thickness is constant ($Q = Q_0 =$ const), the coefficient $D(x)$

$$D(x) = \frac{Q_0 x_0}{(q+1/2)c_0}\left[\left(\frac{x}{x_0}\right)^{\frac{1}{2}} - \left(\frac{x}{x_0}\right)^{\frac{1}{4}-\frac{q}{2}}\right]$$
$$= \frac{2mQ_0 x_0}{(3m+2)c_0}\left[\left(\frac{x}{x_0}\right)^{\frac{1}{2}} - \left(\frac{x}{x_0}\right)^{\frac{1}{4}-\frac{m+1}{2m}}\right], \quad (28)$$

increases at large distances as $x^{1/2}$ for all kinds of bay geometry with the coefficient depending on the cross-section (Fig. 8).

If landslide thickness is decreasing, for example, as $Q \sim c^{-1}$, which bounds the volume of the landslide, coefficient $D(x)$

$$D(x) = \frac{Q_0 x_0}{(q-1/2)c_0}\left[1 - \left(\frac{x}{x_0}\right)^{\frac{1}{4}-\frac{q}{2}}\right]$$
$$= \frac{2mQ_0 x_0}{(m+2)c_0}\left[1 - \left(\frac{x}{x_0}\right)^{\frac{1}{4}-\frac{m+1}{2m}}\right], \quad (29)$$

asymptotically tends to a constant value for all kinds of linearly inclined bay geometry, which is different for different types of bay cross-section (Fig. 9). It can be shown that when $m = 2$ and $Q_0 = A_0$ Eq. (29) coincides with the coefficient in Eq. (19).

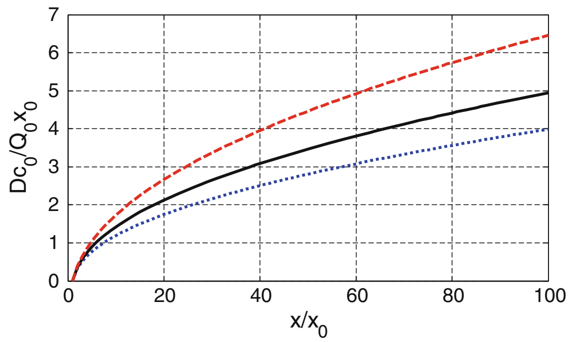

Figure 8
Wave amplitude variation versus distance (Eq. 28) for inclined bays of triangular (*blue dotted line*), parabolic (*black solid line*), and rectangular (*red dashed line*) cross-sections (Q = const)

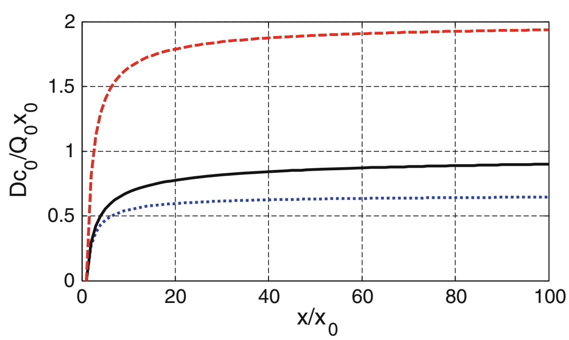

Figure 9
Wave amplitude variations versus distance (Eq. 29) for inclined bays of triangular (*blue dotted line*), parabolic (*black solid line*), and rectangular (*red dashed line*) cross-section ($Q \sim c^{-1}$)

If the landslide thickness decreases significantly, for example, as $Q \sim c^{-2}$, which corresponds to the decrease in the landslide volume, coefficient $D(x)$:

$$D(x) = \begin{cases} \frac{Q_0 x_0}{(q-3/2)c_0}\left[\left(\frac{x}{x_0}\right)^{-\frac{1}{2}} - \left(\frac{x}{x_0}\right)^{\frac{1}{4}-\frac{q}{2}}\right] = \frac{2mQ_0 x_0}{(2-m)c_0}\left[\left(\frac{x}{x_0}\right)^{-\frac{1}{2}} - \left(\frac{x}{x_0}\right)^{\frac{1}{4}-\frac{m+1}{2m}}\right], & m \neq 2 \\ \frac{Q_0 x_0}{2c_0}\left(\frac{x}{x_0}\right)^{-\frac{1}{2}} \ln\frac{x}{x_0}, & m = 2 \end{cases}, \quad (30)$$

varies non-monotonically for all the bay geometries considered (Fig. 10). In particular, the wave amplitude reaches its maximum value at the distance:

$$\frac{x_*}{x_0} = \begin{cases} (q-1/2)^{-(q-3/2)/2}, & q \neq 3/2 \\ e^2, & q = 3/2 \end{cases}. \quad (31)$$

Maximum wave amplitude depends on the cross-section factor, m. For instance, for a U-shaped bay ($m = 2$, $q = 3/2$), it is:

$$D_{\max} = \frac{Q_0 x_0}{e c_0}. \quad (32)$$

All calculations above were performed using the thickness of the landslide as the main variable. The volume of the landslide can be found as a function of its thickness:

$$V = \int z_b^q dx = \int \frac{Q^q(\tau)}{c(\tau)} Z^q(\tau - t) d\tau, \quad (33)$$

where the integral in Eq. (33) is over landslide length. In particular, for relatively short landslides:

$$V(x) \sim \frac{Q^q(x)}{c(x)}. \quad (34)$$

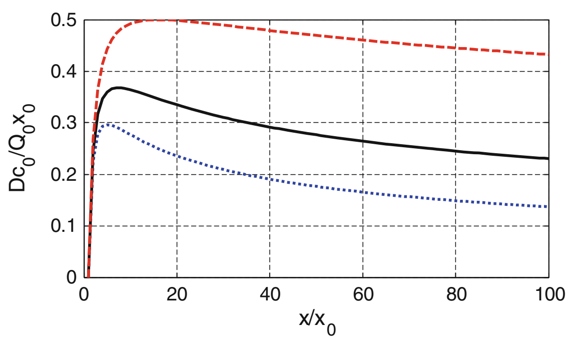

Figure 10
Wave amplitude variations versus distance (Eq. 30) for inclined bays of triangular (*blue dotted line*), parabolic (*black solid line*), and rectangular (*red dashed line*) cross-section ($Q \sim c^{-2}$)

For instance, for the latter case of landslide motion with $Q \sim c^{-2}$ moving along a U-shaped bay ($m = 2$) $V(x) \sim c^{-4} \sim h^{-2}$.

Thus, we demonstrate that the joint action of the resonance and increasing cross-section of the bay may lead to a slow increase of wave amplitude (Fig. 9) or non-monotonic variations of wave amplitude with distance (Fig. 10). The result is sensitive to landslide thickness variations in time and the amplification zone decreases with decreasing landslide thickness.

5. Conclusions

We propose a simple model of landslide tsunami generation in narrow bays and channels. It is based on shallow-water equations averaged over the bay cross-section with an assumption of uniform landslide body surface in the transverse direction of the bay, and small landslide thickness compared with water depth. As a result, the equivalent 1D inhomogeneous wave equation is derived.

The process of landslide tsunami wave generation in inclined bays of specific nonreflecting bottom configurations was studied. The inhomogeneous variable-coefficient wave equation was reduced to the inhomogeneous constant-coefficient wave equation, and its rigorous solution had the form of the Duhamel integral. For a landslide of variable height moving with the constant Froude number, the analytical solution can be presented in an explicit form. Three different bottom configurations (V-shaped bay, U-shaped bay, and a bay of rectangular cross-section) were considered. It was shown that in the resonant case the wave amplitude is bounded for all nonreflecting bottom configurations. However, wave amplitudes depend on the bottom configuration. For example, the offshore-going resonant wave was larger in a bay of rectangular cross-section whereas the onshore going wave was more strongly amplified in a V-shaped bay.

Resonance between landslide motion and wave propagation in linearly inclined bays of variable cross-section was studied, assuming smooth bottom variations. Effects of erosion and accretion of the landslide body were included in the model. It was shown that if the volume of the landslide increases with distance, the wave amplitude also grows, but more slowly than in a bay of constant depth. For a landslide of constant volume, wave amplitude tends to a constant value depending on the cross-section factor of the bay. If the landslide thickness decreases substantially with distance, the amplitude of the generated wave varies non-monotonically and its maximum is also determined by the bay cross-section.

Our analytical solutions can be used for testing numerical codes and for better understanding of the physics of landslide-generated tsunamis.

Acknowledgments

This research was supported by the European Union through the European Regional Development Fund. Partial support from targeted financing by the Estonian Ministry of Education and Research (grant SF0140 007s11), the Estonian Science Foundation (grant 8870), the RFBR (grants 11-05-00216 and 11-02-00483), and the MK (grant 1440.2012.5) is also gratefully acknowledged. ID acknowledges the support provided by the Alexander von Humboldt Foundation.

References

Altinok, Y., Tinti, S., Alpar, B., Yalciner, A.C., Ersoy, S., Bortolucci, E., and Armigliato, A. 2001. *The tsunami of August 17, 1999 in Izmit Bay, Turkey*, Natural Hazards, *24*, 133–146.

Assier-Rzadkiewicz, S., Heinrich, P., Sabatier, P.C., Savoyer, B., and Bourillet, J.F. 2000. *Numerical modeling of a landslide-generated tsunami: the 1979 Nice event*, Pure Appl. Geophys., *157*, 1707–1727.

Bardet, J.P., Synolakis, C.E., Davies, H.L., Imamura, F., and Okal, E.A. 2003. *Landslide tsunamis: Recent findings and research directions*, Pure Appl. Geophys., *160* (10–11), 1793–1809.

Courant, R., and Hilbert, D. 1989. *Methods of Mathematical Physics*. John Wiley & Sons Inc, 598.

Didenkulova, I., Nikolkina, I., and Pelinovsky, E. 2011. *Resonant amplification of tsunami waves generated by an underwater landslide*, Doklady Earth Sci., *436*(1), 66–69.

Didenkulova, I., Nikolkina, I., Pelinovsky, E., and Zahibo, N. 2010. *Tsunami waves generated by submarine landslides of variable volume: analytical solutions for a basin of variable depth*, Nat. Hazards Earth Syst. Sci., *10*, 2407–2419.

Didenkulova, I., and Pelinovsky, E. 2009. *Non-dispersive traveling waves in strongly inhomogeneous water channels*, Phys. Lett. A, *373* (42), 3883–3887.

Didenkulova, I., and Pelinovsky, E. 2010. *Traveling water waves along a quartic bottom profile*, Proc. Estonian Acad. Sci., *59*(2), 166–171.

Didenkulova, I., and Pelinovsky, E. 2011a. *Runup of tsunami waves in U-shaped bays*, Pure Appl. Geophys., *168*(6–7), 1239–1249.

Didenkulova, I., and Pelinovsky, E. 2011b. *Nonlinear wave evolution and runup in an inclined channel of a parabolic cross-section*, Phys. Fluids, *23*(8), 086602, doi:10.1063/1.3623467.

Didenkulova, I., Pelinovsky, E., and Soomere, T. 2008. *Exact travelling wave solutions in strongly inhomogeneous media*, Estonian Journal of Engineering, *14*(3), 220–231.

Didenkulova, I., Pelinovsky, E., and Soomere, T. 2009. *Long surface wave dynamics along a convex bottom*, J Geophys Res Oceans, *114*, C07006. doi:10.1029/2008JC005027.

Di Risio, M., and Sammarco, P. 2008. *Analytical Modeling of Landslide-Generated Waves*, J. Waterway, Port, Coastal, Ocean Eng., *134*(1), 53–60.

Fine, I.V., Rabinovich, A.B., Bornhold, B.D., Thomson, R.E., and Kulikov, E.A. 2005. *The Grand Banks landslide-generated tsunami of November 18, 1929: preliminary analysis and numerical modeling*, Marine Geology, *215*, 45–57.

Fritz, H.M., Mohammed, F., and Yoo, J. 2009. *Lituya Bay landslide impact generated mega-tsunami 50(th) anniversary*, Pure Appl. Geophys., *166* (1–2), 153–175.

Grimshaw, R., Pelinovsky, D., and Pelinovsky, E. 2010. *Homogenization of the variable—speed wave equation*, Wave Motion, *47* (8), 496–507.

Gusiakov, V.K. 2009. Tsunami history: recorded, The Sea. Tsunamis (edited by A. R obinson, E. Bernard), Harvard University Press, Cambridge, 23–54.

Harbitz, C.B., Pedersen, G., and Gjevik, B. 1993. *Numerical simulation of large water waves due to landslides*, J. Hydraulic Eng., *119*, 1325–1342.

Heinrich, P., Guibourg, S., Mangeney, A., and Roche, R. 1999. *Numerical modeling of a landslide-generated tsunami following a potential explosion of the Montserrat volcano*, Phys. Chem. Earth (A), *24* (2), 163–168.

Imamura, F., and Gica, E.C. 1996. *Numerical model for tsunami generation due to subaqueous landslide along a coast*, Science of Tsunami Hazards, *14* (1), 13–28.

Keating, B.H., Waythomas, C.F., and Dawson, A.G. 2000. *Landslides and Tsunamis*, Pure Appl. Geophys., *157*, 871–1313.

Kuo, C.Y., Tai, Y.C., Bouchut, F., Mangeney, A., Pelanti, M., Chen, R.F., and Chang, K.J. 2008. *Simulation of Tsaoling landslide, Taiwan, based on Saint Venant equations over general topography*, Engineering Geology, doi:10.1016/j.enggeo.2008.10.003.

Liu, P.L.-F., Lynnett, P., and Synolakis, C.E. 2003. *Analytical solutions for forced long waves on a sloping beach*, J. Fluid Mech., *478*, 101–109.

LIU, P.L.-F., WU, T.R., RAICHLEN, F., SYNOLAKIS, C.E., and BORRERO, J.C. 2005. *Runup and rundown generated by three-dimensional sliding masses*, J. Fluid Mech., *536*, 107–144.

MANGENEY, A., HEINRICH, P.H., RACHEL, R., BOUDON, G., and CHEMINEE, J.L. 2000. *Modeling of debris avalanche and generated water waves: Application to real and potential events in Montserrat*, Phys Chem Earth (A), *25* (9–11), 741–745.

MCSAVENEY, M.J., GOFF, J.R., DARBY, D.J., GOLDSMITH, P., BARNETT, A., ELLIOTT, S., and NONGKAS, M. 2000. *The 17 July 1998 tsunami, Papua New Guinea: Evidence and initial interpretation*. Marine Geology, *170*, 81–92.

MEI, C.C. 1989. *The Applied Dynamics of Ocean Surface Waves*, World Sci., Singapore, *740*.

NOVIKOVA, L.E., and OSTROVSKY, L.A. 1978. *Excitation of tsunami waves by a travelling displacement of the ocean bottom*, Marine Geodesy, *2*, 365–380.

OKAL, E.A., FRYER, G.J., BORRERO, J.C., and RUSCHER, C. 2002. *The landslide and local tsunami of 13 September 1999 on Fatu Hiva (Marquesas islands; French Polynesia)*, B. Soc. Géol. Fr., *173* (4), 359–367.

OKAL, E.O., and SYNOLAKIS, C.E. 2003. *Theoretical comparisons of tsunamis from dislocations and slides*, Pure Appl. Geophys., *160*, 2177–2188.

PELINOVSKY, E.N. 1996. *Hydrodynamics of tsunami waves*, Institute of Applied Physics, Nizhny Novgorod (in Russian).

PELINOVSKY, E., and POPLAVSKY, A. 1996. *Simplified model of tsunami generation by submarine landslides*, Phys. Chem. Earth, *21*, 13–17.

PUDASAINI, S.P., and HUTTER, K. 2007. *Avalanche Dynamics: Dynamics of Rapid Flows of Dense Granular Avalanches*, Springer, 602.

RANGUELOV, B., TINTI, S., PAGNONI, G., TONINI, R., ZANIBONI, F., and ARMIGLIATO, A. 2008. *The nonseismic tsunami observed in the Bulgarian Black Sea on 7 May 2007: Was it due to a submarine landslide*? Geophys. Res. Lett., *35* (18), L18613.

SAMMARCO, P., and RENZI, E. 2008. *Landslide tsunamis propagating along a plane beach*, J. Fluid Mech., *598*, 107–119.

SYNOLAKIS, C.E. 1991. *Green law and the evolution of solitary waves*. Phys. Fluids, *3* (3), 490–491.

SYNOLAKIS, C.E., BARDET, J., BORRERO, J.C., DAVIES, H.L., OKAL, E.A., SILVER, E.A., SWEET, S., and TAPPIN, D.R. 2002. *The slump origin of the 1998 Papua New Guinea Tsunami*, Proc. R. Soc. Lond. A, *458*, 763–789.

TINTI, S., and BORTOLUCCI, E. 2000. *Analytical investigation of tsunamis generated by submarine slides*, Annali di Geofisica, *43*, 519–536.

TINTI, S., BORTOLUCCI, E., and CHIAVETTIERI, C. 2001. *Tsunami excitation by submarine slides in shallow-water approximation*, Pure Appl. Geophys., *158*, 759–797.

TINTI, S., PAGNONI, G., and ZANIBONI, F. 2006. *The landslides and tsunamis of the 30th of December 2002 in Stromboli analysed through numerical simulations*, Bull. Volcanol., *68*, 462–479.

WARD, S.N. 2001. *Landslide tsunami*, J. Geophys. Res., *106*, 11201–11215.

YALCINER, A.C., PELINOVSKY, E.N., OKAL, E., and SYNOLAKIS, C.E. 2003. *Submarine landslides and tsunamis*. NATO Science Series: IV. Earth and Environmental Sciences, 21, Kluwer.

(Received January 9, 2012, revised May 8, 2012, accepted May 25, 2012, Published online July 7, 2012)